http://dx.doi.org/10.5012/bkcs.2014.35.8.2304

Synthesis and *In vivo* Evaluation of 5-Methoxy-2-(phenylethynyl)quinoline (MPEQ) and [^{11}C]MPEQ Targeting Metabotropic Glutamate Receptor 5 (mGluR5)

Ji Young Kim,[†,‡] Myung-Hee Son,[†,§] Kihang Choi,[‡] Du-Jong Baek,[§] Min Kyung Ko,[†] Eun Jeong Lim,[†] Ae Nim Pae,[†,#] Gyochang Keum,[†,#] Jae Kyun Lee,[†] Yong Seo Cho,[†,#] Hyunah Choo,[†,#] Youn Woo Lee,[¶] Byung Seok Moon,[¶] Byung Cheol Lee,[¶] Ho-Young Lee,[¶,$,*] and Sun-Joon Min[†,#,*]

[†]*Center for Neuro-Medicine, Brain Science Institute, Korea Institute of Science and Technology (KIST), Seoul 136-791, Korea. [*]E-mail: sjmin@kist.re.kr*
[‡]*Department of Chemistry, Korea University, Seoul 136-701, Korea*
[§]*Department of Chemistry, College of Natural Sciences, Sangmyung University, Seoul 110-743, Korea*
[#]*Department of Biological Chemistry, University of Science and Technology (UST), Daejeon 305-333, Korea*
[¶]*Department of Nuclear Medicine, Seoul National University Bundang Hospital, Seongnam 463-707, Korea*
[$]*Cancer Research Institute, Seoul National University, Seoul 110-779, Korea. [*]E-mail: debobkr@gmail.com*
Received April 10, 2014, Accepted April 15, 2014

The synthesis and *in vivo* evaluation of 5-methoxy-2-(phenylethynyl)quinoline (MPEQ) **3** as a potential mGluR5 selective radioligand is described. We have identified MPEQ **3** exhibiting the analgesic effect in the neuropathic pain animal model. The effect of mGluR5 on neuronal activity in rat brain was evaluated through FDG/PET imaging in the presence of MPEQ **3**. In addition, the PET study of [^{11}C]MPEQ **3** proved that accumulation of [^{11}C]MPEQ **3** in rat brain was correlated to the localization of the mGluR5.

Key Words : MPEQ, Metabotropic glutamate receptor 5 (mGluR5), *in vivo*, PET imaging, Neuropathic pain

Introduction

Glutamate is the major excitatory neurotransmitter in the central nervous system (CNS) and regulates signal transmission between neurons through diverse sets of receptors.[1] The metabotropic glutamate receptors (mGluR) belong to the subfamily class C of G-protein coupled receptors (GPCRs). They consist of eight subtypes, which have been divided into three groups based on their structural similarity, localization and signaling pathway. mGluR5, one of the Group I receptors, is mainly expressed in brain regions. This receptor has been implicated in a variety of neurological and psychiatric disorders such as anxiety disorders,[2] schizophrenia,[3] Parkinson's disease,[4] fragile X syndrome,[5] and neuropathic pain.[6] Given the importance of mGluR5 in such disease states, *in vivo* evaluation of mGluR5 in the CNS would validate the role of this receptor in physiological and pathological conditions. Thus, potent and selective mGluR5 radioligands could provide valuable tools for monitoring disease progression as well as evaluating the pharmacokinetics of therapeutics.

During the past decade, a large number of radioligands have been identified as PET tracer candidates for visualization of glutamate receptors *in vivo*.[7] However, only a limited number have been successfully used in *in vivo* studies. Among the mGluR5 PET tracers, [^{11}C]ABP-688 (**1**) turned out to be the most successful radioligand for PET imaging, demonstrating relatively high ligand uptake in mGluR5-rich brain regions such as the anterior cingulate, medial temporal lobe, amygdala, caudate and putamen.[8]

In parallel to our discovery project aiming at development of mGluR5 negative allosteric modulators (NAMs) for treatment of neuropathic pain, we further extended our study to indentify a PET tracer, which will allow us to better understand mGluR5 and its role in neuropathic pain. Recently, we reported that 2-alkynylquinoline **2** exhibited favorable analgesic effects in spinal nerve ligation (SNL) model of neuropathic pain.[9] This result suggested that a radiotracer based on this chemical structure would be suitable for measuring its brain uptake and distribution, which is useful for elucidating the effect of mGluR5 on neuronal activity in the brain of rat neuropathic pain model.

Due to a lack of labeling substituents on compound **2**, we investigated *in vitro* inhibitory activity of other analogues against mGluR5. Considering the several candidates, we

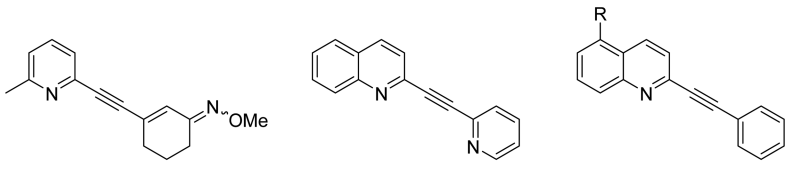

ABP688 (1) **2** **3** (R = OMe)
4 (R = F)

Figure 1. Structures of **1** (ABP688), **2**, **3** (MPEQ) and **4**.

Table 1. *In vitro* inhibitory activity and safety profile of 2-alkynylquinolines **3** and **4**

Compds	% Inhibition ($mGluR_5$)[a]		% Inhibition ($mGluR_1$)[a]		$mGluR_5$ IC_{50} (μM)
	10 μM	1 μM	10 μM	1 μM	
3 (MPEQ)	68.03	63.58	12.05	–4.73	0.41 ± 0.07
4	65.17	28.20	16.24	2.13	–

[a]Ca^{2+} flux assay using glutamate as agonist.

have selected compounds **3** and **4** containing either methoxy group or fluorine at the 5-position of quinoline, which would be easily converted to their corresponding PET ligands. Based on the *in vitro* activities of both compounds (Table 1), 5-methoxy-2-(phenylethynyl)quinoline **3** (**MPEQ**) was identified as a relevant radioligand candidate with regard to potency and selectivity. Herein, we report on the *in vitro* pharmacological characteristic of MPEQ as an mGluR5 antagonist and its preliminary evaluation for labeling mGluR5 *in vivo* in living rats.

Result and Discussion

The synthesis of compound **3** and its labeling precursor **9** started from commercially available 5-hydroxyquinoline **5**. Methylation of **5** with $TMSCHN_2$ gave 5-methoxyquinoline **6a**, which was converted to 2-chloroquinoline derivative **7a** *via N*-oxidation and chlorination. The Sonogashira reaction of **7a** with phenylacetylene produced the target quinoline **3** in 50% yield. Next, we were able to synthesize the precursor **9** by using the similar reaction sequences. Thus, hydroxyquinoline **5** was protected as pivaloate **6b**, which was subjected to chlorination and alkynylation to afford 2-alkynylquinoline **7b**. Finally, removal of pivaloyl group was performed by $LiAlH_4$ reduction to give the corresponding 5-hydroxy-2-alkynyl quinoline **9** in good yield (Scheme 1).

Methylation reactions of the precursor **9** are summarized in Table 2. Initially, we treated compound **9** with dimethylsulfate in the presence of potassium carbonate for 1 h to obtain **3** in 31% yield. However, it is necessary to reduce the reaction time within 30 min to generate reasonable amount of PET probes. We performed further optimization using methyl iodide as an electrophile. The reaction of **6** with methyl iodide and tetrabutylammonium hydroxide in methanol at 50 °C in 15 min yielded the target compound **3** in 47% yield. Therefore, we decided to attempt incorporation of a [^{11}C] methyl group to form the ^{11}C-labeled MPEQ **3** under this optimized condition.

Table 2. Optimization of methylation reaction

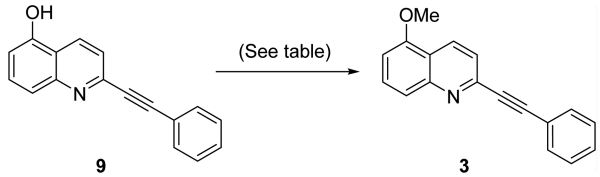

9 **3**

Entry	Condition	Time (h)	Yield
1	Me_2SO_4, K_2CO_3, acetone, rt	1	31%
2	MeI, KOH, MeOH, 50 °C	0.5	56%
3	MeI, TBAH, MeOH, 50 °C	0.25	47%

[^{11}C]MPEQ **3** was synthesized from **9** by [^{11}C]methylation using [^{11}C]CH_3I in the TRACERlab FX C-pro module (GE Healthcare). [^{11}C]CO_2 was produced at the KOTRON-13 cyclotron (Samyoung Unitech Co., Korea) by irradiation of a gas target containing N_2 (99.9999%) using the $^{14}N(p,a)^{11}C$ nuclear reaction. [^{11}C]CH_3I, converted from [^{11}C]CO_2 using the gas phase conversion in an automated module, was bubbled by a flow of He gas into a solution of acetone (0.4 mL) containing **9** (1 mg) and tetrabutylammonium hydroxide (40 wt % solution in water, 1.5 μL) at –20 °C. When radioactivity had peaked, the solution was heated to 70 ºC and kept at this temperature for 4 min. After cooling down to room temperature by He flow, the reaction mixture was quenched by addition of water (1.4 mL) and subsequently transferred to the 2 mL of injection loop of HPLC system. The reaction mixture was purified by reverse phase HPLC (Waters, Xterra RP-18, 10 μm, 10 × 250 mm with guard column (10 × 10 mm); eluent: 70% CH_3CN/H_2O; flow rate: 3 mL/min) equipped with a gamma-ray detector and a UV detector at 254 nm (Figure 2). The desired fraction of [^{11}C]MPEQ **3** collected from HPLC at around 11.7 min was diluted with 40 mL of water. The resulting solution was then

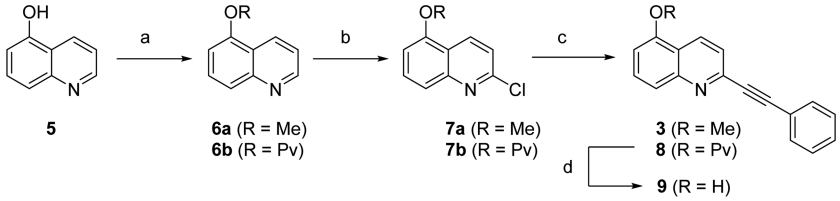

Scheme 1. Reagents and conditions: (a) $TMSCHN_2$, MeOH, rt, 42% (R = Me) or PvCl, pyr, CH_2Cl_2, 84% (R = Pv); (b) i) *m*CPBA, DCM, 0 °C to rt; ii) $POCl_3$, CH_2Cl_2, reflux, 32% (R = Me) or 37% (R = Pv); (c) phenylacetylene, $PdCl_2(PPh_3)_2$, CuI, Et_3N, 80 °C, 50% (R = Me) or 100% (R = Pv); (d) $LiAlH_4$, THF, 0 °C to rt, 49%.

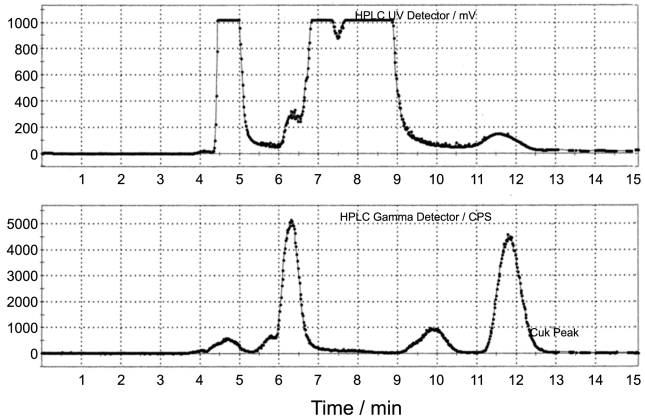

Figure 2. Representative HPLC profile from the TRACERlab FX C-pro module (upper: UV-254 nm; bottom: gamma-ray).

loaded into a C18 plus Sep-Pak cartridge to trap only [^{11}C]MPEQ **3** and to remove the HPLC solvent. After rinsing the cartridge with 10 mL of water, the pure product was eluted with 1.5 mL of ethanol and 16 mL of saline for adjustment of 8.5% ethanol/saline. Consequently, the isolated radiochemical yield was 19.1 ± 4.9% (n = 6, decay corrected) and produced approximately 1.7-2.2 GBq per batch. An aliquot of the formulated solution was checked by analytical HPLC (Waters, Xterra RP-18, 5 μm, 3.9 × 250 mm; eluent: 70% CH_3CN/H_2O; flow rate: 1 mL/min) for radiochemical identity (Figure 2), radiochemical purity and specific activity. The radiochemical purity was over 99% and specific radioactivity was 137 ± 52 GBq/μmol at the end of synthesis.

After establishing the synthesis of the labeled compound **3**, the pharmacokinetic parameters for **3** following intravenous and oral administration in rats are determined as shown in Table 3. Although compound **3** has high value of the mean volume distribution, it showed relatively good exposure and oral bioavailability. In particular, the brain to plasma ratios in intravenous and oral administration were significantly high, which indicated that MPEQ **3** has excellent characteristics of brain penetration.

The *in vivo* efficacy of **3** was further evaluated in the rat neuropathic pain model developed by Chung *et al.* (Figure 3).[10] In order to induce a neuropathic pain state to rats, tight ligation of the L5 spinal nerve at a site distal to the dorsal root ganglion (DRG) was executed. After surgical operation, the pain was fully stimulated for 14 days and behavioral tests for mechanical allodynia and cold allodynia were performed. The rats were treated orally with 100 mg/kg of **3** or gabapentin (a positive control). In fact, MPEQ **3** exhibited highest analgesic effect in both behavior tests at 3 h. Although the *in vivo* efficacy of **3** is not as high as that of gabapentin in this behavior test, we believed that it was effective enough to investigate *in vivo* imaging targeting mGluR5 in the rat neuropathic pain model.

To evaluate the effect of MPEQ **3** in cerebral neuronal activity, we acquired [^{18}F] fluorodeoxyglucose (FDG) PET/CT image of five Sprague Dawley (SD) rats with and without intravenous administration of compound **3**. Practically, MPEQ **3** was intravenously administrated to rats 30 minutes prior to FDG injection and the PET/CT image was acquired 60 minutes after FDG injection. Each image was spatially normalized to rat template image and compared the images obtained with and without administration of **3** were compared using statistical parametric mapping 5 (SPM5), by paired t-test (uncorrected $p < 0.001$ with permutation 10,000). Based on this experiment, we verified that MPEQ **3** significantly decreased regional glucose metabolism in both primary somatosensory cortices (Figure 4).

Next, we evaluated the effect of **3** in the neuropathic pain rat model by the acquisition of FDG PET/CT image with and without intravenous administration and compared the

Table 3. Mean (± SD[a]) pharmacokinetic parameters after intravenous (n = 5) administration and oral (n = 5) administration (10 mg/kg) of MPEQ (**3**) to SD male rats

Plasma	Intravenous	Oral
$AUC_{0-\infty}$ (μg min/mL)	272.86 ± 30.21	99.21 ± 17.42
AUC_{last} (μg min/mL)	250.60 ± 22.54	84.97 ± 21.59
Terminal half-life (min)	170.68 ± 28.52	158.44 ± 88.8
C_{max} (μg/mL)	–	0.43 ± 0.25
T_{max} (min)	–	66 (30-120)[b]
CL (mL/mim/kg)		–
MRT (min)		–
V_{ss} (mL/kg)	36.99 ± 3.85	–
Ae (%)	98.12 ± 13.47	0.12
Plasma conc (μg/mL) @ 2 h	0.48 ± 0.05	0.31 ± 0.13
Plasma conc (μg/mL) @ 8 h	0.09 ± 0.03	0.05 ± 0.02
Brain conc (μg/mL) @ 2 h	1.26 ± 0.15	0.84 ± 0.24
Brain-to-plasma ratio (B/P) @ 2 h	2.67	3.03
F (%)		36.4

Values are presented as mean (standard deviation in parentheses). $AUC_{0-\infty}$, total area under the plasma concentration–time curve from time zero to time infinity; AUC_{last}, total area under the plasma concentration–time curve from time zero to last measured time; C_{max}, peak plasma concentration; T_{max}, time to reach C_{max}; CL, time-averaged total body clearance; MRT, mean residence time; V_{ss}, apparent volume of distribution at steady state; *Ae*, Excreted amount; *F*, bioavailability; [a]SD: Standard deviations; [b]Median (range) for T_{max}

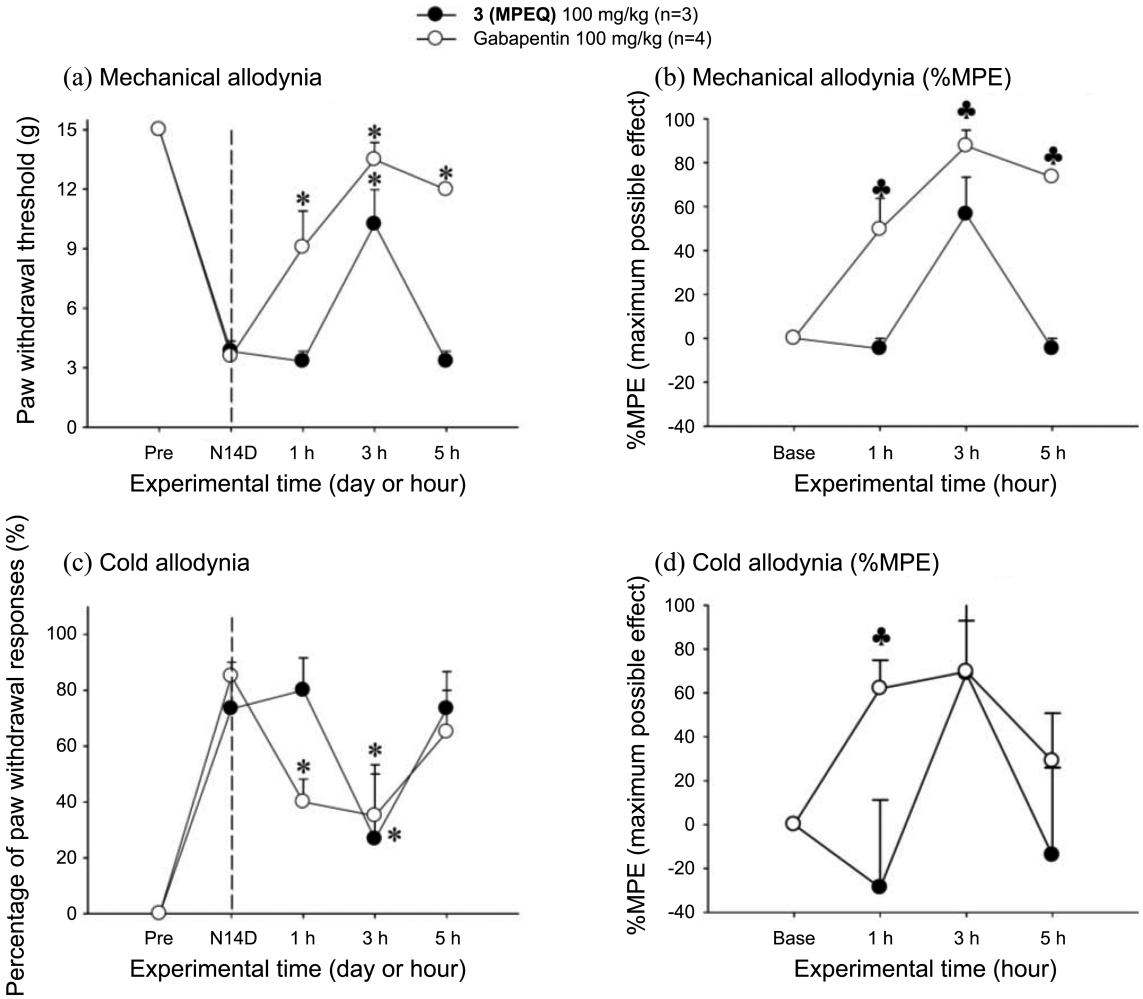

Figure 3. Effect on mechanical allodynia (a and b) and cold allodynia (c and d) after oral administration of gabapentin (○, 100 mg/kg, n = 4) and **3** (●, 100 mg/kg, n = 3) to neuropathic pain-induced rats. Experimental time expressed as D for days after neuropathic injury (N) and h for hours after gabapentin or **3** administration, *$P < 0.05$ (gabapentin), $^{*}P < 0.05$ (**3**) *vs* pre-administration value (paired *t*-test), ♣$P < 0.05$ gabapentin *vs* **3** (unpaired *t*-test).

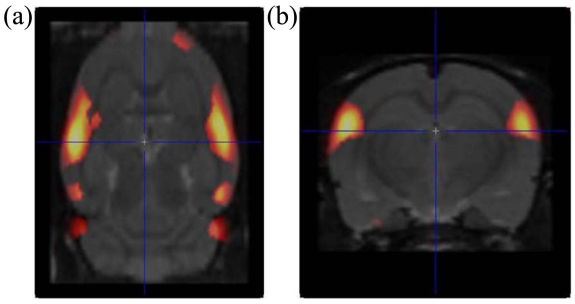

Figure 4. Comparison FDG PET/CT of normal SD rat with and without MPEQ **3** administration. (a) transaxial view of rat brain (b) coronal view of rat brain. Colored lesions represent the area with significantly lower neuronal activity after MPEQ 3 administration. Those areas are the both somatosensory cortices (uncorrected u < 0.001 with permutation 10,000).

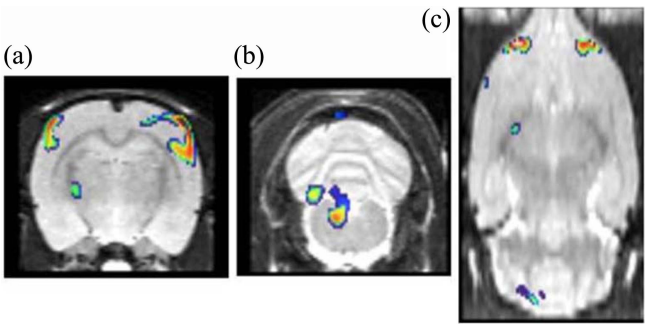

Figure 5. Comparison FDG PET/CT of neuropathic model rat with and without administration of **3**. Neuronal activity was reduced in the sensory motor region (a), PAG (periaqueductal gray) region (b, c) and left thalamus (a, c) that are known as related to the neuropathic pain pathway (uncorrected u < 0.001 with permutation 10,000).

different states (Figure 5). After intravenous administration of **3**, reduction of neuronal activity was observed in the sensory motor region, PAG (periaqueductal gray) region and left thalamus that are associated with the neuropathic pain pathway.[11] Taken together with the *in vitro* data (Figure 3), this result indicated that MPEQ **3** exhibited the analgesic effect in the SNL rat model by modulating the pain signaling

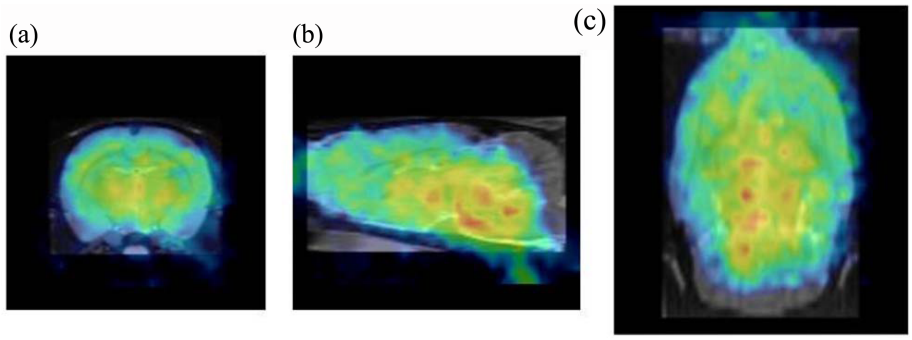

Figure 6. Summation image of [^{11}C]MPEQ **3** dynamic PET/CT image. (a) coronal image (b) sagittal image (c) transaxial image of [^{11}C]MPEQ **3** dynamic PET/CT image. [^{11}C]MPEQ **3** well penetrates blood brain barrier. [^{11}C]MPEQ **3** distributed in cerebal cortex and mid brain area. However, there is low uptake in the cerebellum that is known as area with lower mGluR5 expression.

pathway through mGluR5 antagonism.

Finally, the possibility of [^{11}C]MPEQ **3** as a probe for imaging the mGuR5 is examined by analysis of brain PET imaging. Following the procedure described above, [^{11}C]MPEQ **3** was prepared and intravenously injected to normal rats. Subsequent dynamic PET image was acquired until 90 minutes (Figure 6). The PET study of [^{11}C]MPEQ **3** in rat brain revealed that it effectively penetrated blood brain barrier (BBB). In particular, accumulation of [^{11}C]MPEQ **3** in rat brain was correlated to the localization of the mGluR5. We observed relatively high level of [^{11}C]MPEQ **3** uptake in the cerebral cortex, olfactory tubercle, hippocampus and striatum. On the other hand, the cerebella uptake was considerably low, which supports the evidence that there is low mGluR5 expression in the cerebellum region as reported in the previous literature.[12]

Conclusion

In this study, we synthesized 5-methoxy-2-(phenylethynyl)quinoline (MPEQ) **3** as a potential mGluR5 selective radioligand. The *in vivo* evaluation of MEPQ **3** in the SNL model turned out that it showed significant analgesic effect in behavior tests of mechanical allodynia and cold allodynia. The reduction of neuronal activity in sensory motor region of the neuropathic pain animal model was observed by FDG/PET imaging variation before and after treatment of MPEQ **3**. In addition, the PET study of [^{11}C]MPEQ **3** proved that [^{11}C]MPEQ **3** was highly localized in the mGluR5 rich region of rat brain. Although MPEQ **3** showed possibility as an mGluR5 radiotracer, it should be further optimized as an accurate radiotracer, which is useful for quantitative evaluation of mGluR5 biodistribution.

Experimental Section

General. All reactions were carried out under dry nitrogen unless otherwise indicated. Commercially available reagents were used without further purification. Solvents and gases were dried according to standard procedures. Organic solvents were evaporated with reduced pressure using a rotary evaporator. Analytical thin layer chromatography (TLC) was performed using glass plates precoated with silica gel (0.25 mm). TLC plates were visualized by exposure to UV light (UV), and then were visualized with a *p*-anisaldehyde stain followed by brief heating on hot plate. Flash column chromatography was performed using silica gel 60 (230-400 mesh, Merck) with the indicated solvents. ^{1}H and ^{13}C spectra were recorded on Bruker 300, Bruker 400 or Varian 300 NMR spectrometers. ^{1}H NMR spectra are represented as follows: chemical shift, multiplicity (s = singlet, d = doublet, t = triplet, q = quartet, m = multiplet), integration, and coupling constant (J) in Hertz (Hz). ^{1}H NMR chemical shifts are reported relative to $CDCl_3$ (7.26 ppm). ^{13}C NMR was recorded relative to the central line of $CDCl_3$ (77.0 ppm). GC/MS and LC/MS analyses were respectively performed on Agilent 6890N Network Gas system with 5793N MSD and Applied Biosystems/MDS SCIEX API3200 LC/MS/MS system.

5-Methoxyquinoline (6a):[13] To a solution of 5-quinolinol **5** (164 mg, 1.13 mmol) in MeOH (7 mL) cooled to 0 °C was slowly added trimethylsilyldiazomethane (6 mL, 0.5 M in Et_2O). The reaction mixture was allowed to warm to room temperature and stirred for 26 h. After addition of water, the reaction mixture was extracted with ethyl acetate (3 × 15 mL). The combined organic layer was washed with brine, dried over anhydrous $MgSO_4$, and concentrated under reduced pressure. The crude oil was purified by column chromatography on silica gel (EtOAc/CH_2Cl_2/hexane = 1:2:4) to give 5-methoxyquinoline **6a** (76 mg, 42%) as a white solid: ^{1}H NMR ($CDCl_3$, 300 MHz) δ 4.04 (s, 3H), 6.89 (d, J = 7.5 Hz, 1H), 7.41 (q, J = 4.2 Hz, 1H), 7.62-7.74 (m, 2H), 8.61 (dd, J = 8.4, 1.2 Hz, 1H), 8.93 (dd, J = 4.2, 1.8 Hz, 1H).

2-Chloro-5-methoxyquinoline (7a):[13] To solution of 5-methoxyquinoline **6a** (104 mg, 0.66 mmol) in CH_2Cl_2 (3 mL) was added *meta*-chloroperoxybenzoic acid (195 mg, 1.13 mmol) at 0 °C for 30 min. The mixture was allowed to warm to room temperature and stirred for additional 3 h. The reaction is queched with 4 N NaOH and extracted with CH_2Cl_2. The combined organic extracts were washed with brine, dried over anhydrous $MgSO_4$ and concentrated under reduced pressure to give the crude *N*-oxide, which was directly used for the next step without purification. To solution of the resulting *N*-oxide in CH_2Cl_2 (2.5 mL) was adeed

phosphorus oxychloride (0.09 mL, 0.99 mmol). The reaction mixture was refluxed at 60 °C for 3 h, allowed to cool to room temperature and poured into ice-water. The resulting mixture was treated with 4 N aqueous NaOH until pH reached to around 10. The organic phase was extracted with CH_2Cl_2 (3 × 5 mL), washed with brine, dried over anhydrous $MgSO_4$, and concentrated under reduced pressure. The crude residue was purified by column chromatography on silica gel (EtOA/CH_2Cl_2/Hexane = 1:2:4) to give 2-chloro-5-methoxy-chloroquinoline **7a** (40.1 mg, 32%) as a white solid: ^{1}H NMR ($CDCl_3$, 300 MHz) δ 4.01 (s, 3H), 6.88 (dd, *J* = 7.2, 1.5 Hz, 1H), 7.35 (d, *J* = 8.7 Hz, 1H), 7.59-7.67 (m, 2H), 8.51 (d, *J* = 8.7 Hz, 1H).

5-Methoxy-2-(phenylethynyl)quinoline (3): To a solution of 2-chloro-5-methoxyquinoline (12.7 mg, 0.0656 mmole) in THF (1.5 mL) was added $Pd(PPh_3)_4$ (5.3 mg, 0.00459 mmol), CuI (3.3 mg, 0.017 mmol). The reaction mixture was stirred for 5 min and triethylamine (0.5 mL) and phenylacetylene (0.01 mL, 0.131 mmol) were added. After the resulting mixture was stirred at 80 °C for 24 h, it was allowed to cool to room temperature and filtered through a pad of Celite by the aid of EtOAc. The filtrate was treated with water and extracted with EtOAc (3 × 10 mL). The organic layer was washed with water and brine, dried over anhydrous $MgSO_4$, and concentrated under reduced pressure. The crude oil was purified by column chromatography on silica gel (EtOAc/hexane = 1:10) to give 5-methoxy-2-(phenylethynyl)quinoline **3** (8.6 mg, 50%) as a white solid: mp 92-97 °C; ^{1}H NMR ($CDCl_3$, 300 MHz) δ 4.05 (s, 3H), 6.91 (d, *J* = 7.5 Hz, 1H), 7.42-7.44 (m, 3H), 7.62-7.77 (m, 5H), 8.60 (d, *J* = 8.7 Hz, 1H); ^{13}C NMR ($CDCl_3$, 100 MHz) δ 55.8, 89.4, 89.9, 104.8, 119.6, 121.5, 122.2, 123.5, 128.4, 129.1, 130.0, 131.0, 132.3, 143.9, 149.1, 155.0; GC/MS (EI): *m/z*: calcd for $C_{18}H_{13}NO$: 259.10, M^+; found: 259.

Quinolin-5-yl pivalate (6b):[14] To a solution of 5-quinolinol **5** (197.2 mg, 1.36 mmol) in CH_2Cl_2 (2.8 mL) was added pyridine (0.32 mL, 3.97 mmol) and pivaloyl chloride (0.18 mL, 1.5 mmol). The reaction mixture was stirred at room temperature for 17 h and quenched with saturated ammonium chloride. The resulting solution was extracted with EtOAc (3 × 10 mL) and the combined organic layer was washed with brine, dried over $MgSO_4$, and concentrated under reduced pressure. The crude oil was purified by column chromatography on silica gel (EtOAc/hexane = 1:1) to give quinolin-5-yl pivalate **6b** (261.2 mg, 84%) as a white solid: ^{1}H NMR ($CDCl_3$, 300 MHz) δ 1.48 (s, 9H), 7.29 (dd, *J* = 7.6, 0.9 Hz, 1H), 7.42 (dd, *J* = 8.5, 4.2 Hz, 1H), 7.70 (dd, *J* = 8.5, 7.7 Hz, 1H), 8.00-8.03 (m, 1H), 8.17 (qd, *J* = 8.5, 0.8 Hz, 1H), 8.94 (dd, *J* = 4.2, 1.7 Hz, 1H); ^{13}C NMR ($CDCl_3$, 100 MHz) δ 27.2, 39.4, 118.4, 121.2, 122.3, 127.1, 128.7, 129.6, 146.3, 148.8, 150.6, 176.6.

2-Chloroquinolin-5-yl pivalate (7b):[15] Following the same procedure as that used for the synthesis of **7a**, the reaction of **6b** (245 mg, 1.07 mmol), *meta*-chloroperoxybenzoic acid (368 mg, 2.13 mmol), phosphorus oxychloride (0.15 mL, 1.60 mmol) in CH_2Cl_2 (10.0 mL) afforded 2-chloroquinolin-5-yl pivalate **7b** (104 mg, 37%) as a white solid: ^{1}H NMR ($CDCl_3$, 300 MHz) δ 1.48 (s, 9H), 7.31 (dd, *J* = 7.7, 0.9 Hz, 1H), 7.41 (d, *J* = 8.8 Hz, 1H), 7.73 (t, *J* = 8.1 Hz, 1H), 7.92 (d, *J* = 8.6 Hz, 1H), 8.11 (d, *J* = 8.8 Hz, 1H); ^{13}C NMR ($CDCl_3$, 100 MHz) δ 27.3, 39.6, 119.1, 121.1, 122.6, 126.3, 130.2, 132.8, 146.5, 148.5, 151.3, 176.7.

2-(Phenylethynyl)quinolin-5-yl Pivalate (8): Following the same procedure as that used for the synthesis of **3**, the reaction of -chloroquinolin-5-yl pivalate **7b** (23.9 mg, 0.0906 mmol), CuI (3.7 mg, 0.019 mmol), Pd $(PPh_3)_4$ (7.5 mg, 0.000649 mmol), phenylacetylene (0.02 mL, 0.181 mmol) in triethylamine (0.6 mL) gave 2-(phenylethynyl)-quinolin-5-yl pivalate **8** (29.8 mg, 100%) as a white solid: ^{1}H NMR ($CDCl_3$, 400 MHz) δ 1.49 (s, 9H), 7.29 (dd, *J* = 7.6, 0.9 Hz, 1H), 7.36-7.40 (m, 3H), 7.62 (d, *J* = 8.6 Hz, 1H), 7.66-7.69 (m, 2H), 7.72-7.75 (m, 1H), 8.02 (d, *J* = 8.6 Hz, 1H), 8.15 (dd, *J* = 8.7, 0.7 Hz, 1H); ^{13}C NMR ($CDCl_3$, 75 MHz) δ 27.36, 39.59, 89.12, 90.59, 119.10, 121.23, 122.00, 124.60, 127.09, 128.47, 129.35, 129.49, 129.97, 132.33, 144.11, 146.27, 148.92, 176.78; GC/MS (EI): *m/z*: calcd for $C_{21}H_{18}N_2O_2$: 330.14, $[M–H]^+$; found: 329.

2-(Phenylethynyl)quinolin-5-ol (9): To the solution of 2-(phenylethynyl)quinolin-5-yl pivalate **8** (15.4 mg, 0.047 mmol) in THF (0.78 mL) was added lithium aluminum hydride (0.06 mL, 1.0 M in THF) at 0 °C. The reaction was allowed to warm to room temperature and stirred for 30 min. The mixture was quenched with NH_4Cl solution. The resulting mixture was extracted with diethyl ether (3 × 3 mL) and the combined organic layer was washed with water and brine, dried over $MgSO_4$, and concentrated under reduced pressure. The crude oil was purified by column chromatography on silica gel (EtOAc/hexane = 1:1) to give 2-(phenylethynyl)quinolin-5-ol **9** (5.6 mg, 49%) as a yellow solid: ^{1}H NMR (MeOD, 300 MHz) δ 6.92 (d, *J* = 0.84 Hz, 1H), 7.42-7.49 (m, 4H), 7.55-7.68 (m, 4H), 8.66 (d, *J* = 4.3 Hz, 1H); ^{13}C NMR (MeOD, 75 MHz) δ 88.2, 89.9, 108.9, 118.0, 119.1, 121.8, 122.4, 128.4, 129.3, 130.8, 131.7, 132.2, 143.5, 153.5; LC/MS (ESI^+): *m/z*: calcd for $C_{17}H_{12}NO$: 246.09, $[MI+H]^+$; found: 246.2.

***In vivo* Behavioral Test.** Two behavioral tests (mechanical allodynia and cold allodynia) were conducted for rats at 1 day prior to surgery and 14 days after surgery. After the postoperative behavioral test, the animals were treated orally with 100 mg/kg compound **3** or gabapentin. The tests were re-evaluated at 1 h, 3 h, and 5 h after administration.

Mechanical Allodynia. Testing was performed according to methods described previously.[16] Rats were acclimated in a transparent plastic boxes permitting freedom of movement with a wire mesh floor to allow access to the planter surface of the hind paws. A von Frey filament (Stoelting, Wood Dale, IL) was applied 5 times (once every 3-4 s) to hind paw. Von Frey filaments were used to assess the 50% mechanical threshold for paw withdrawal. The 50% withdrawal threshold was determined by using the up-down method and formula given by Dixon[17]: 50% threshold = $10 (X + kd)/10^4$, where X is the value of the final von Frey hair used (in log units), k is the tabular value for the pattern of positive/negative responses modified from Dixon,[17] and d is the mean differ-

ence between stimuli in log units (0.17).

Cold Allodynia. To quantify cold sensitivity of the paw, brisk paw withdrawal in response to acetone application was measured as described previously.[18] The rat was placed under a transparent plastic box on a metal mesh floor and acetone was applied to the plantar surface of the hind paw. To do this, an acetone bubble was formed at the end of a small piece of polyethylene tubing which was connected to a syringe. The bubble was then gently touched to the heel. The acetone quickly spread over the proximal half of the plantar surface of the hind paw. The acetone was applied 5 times to hind paw at 2 min interval. The frequency of paw withdrawal was expressed as a percentage [(no. of trials accompanied by brisk foot withdrawal/total no. of trials) × l00].

Data Analysis. The results of behavioral tests are expressed as a %MPE. For example, paw withdrawal thresholds were converted to %MPE by the following formula, by using a cutoff of 15 g (the threshold for normal rats) to define maximum possible effect: (post drug threshold – baseline threshold)/(cutoff – baseline threshold) × 100. %MPE values near 100 indicate normal mechanical thresholds (*i.e.*, at or near 15 g), whereas values near 0 indicate allodynia. The result of cold allodynia was also expressed as %MPE.

Acknowledgments. This research was supported by a grant of the Korea Health technology R&D Project, the Ministry of Health and Welfare, Republic of Korea (HI11C0998) and by the Korea Institute of Science and Technology (KIST, 2E24670, 2E25023, and 2E24510).

References

1. (a) Pin, J. P.; Duvoisin, R. *Neuropharmacology* **1995**, *34*, 1. (b) Madden, D. R. *Nat. Rev. Neurosci*. **2002**, *3*, 91. (c) Watkins, J. C. *Biochem. Soc. Trans*. **2000**, *28*, 297.
2. (a) Spooren, W. P. J. M.; Vassout, A.; Neijt, H. C.; Kuhn, R.; Gasparini, F.; Roux, S.; Porsolt, R. D.; Gentsch, C. *J. Pharmacol. Exp. Ther*. **2000**, *295*, 1267. (b) Porter, R. H.; Jaeschke, G.; Spooren, W.; Ballard, T. M.; Buttelmann, B.; Kolczewski, S.; Peters, J.-U.; Prinssen, E.; Wichmann, J.; Viera, E.; Muhlemann, A.; Gatti, S.; Mutel, V.; Malherbe, P. *J. Pharmacol. Exp. Ther.* **2005**, *315*, 711. (c) Swanson, C. J.; Bures, M.; Johnson, M. P.; Linden, A. M.; Monn, J. A.; Schoepp, D. D. *Nat. Rev. Drug Disc.* **2005**, *4*, 131.
3. (a) Marino, M. J.; Conn, P. J. *Curr. Drug Targets: CNS Neurol. Disord*. **2002**, *1*, 1. (b) Moghaddam, B. *Psychopharmacology* **2004**, *174*, 39. (c) Conn, P. J.; Lindsley, C. W.; Jones, C. K. *Trends Pharmacol. Sci.* **2009**, *30*, 25.
4. (a) Hsieh, M.-H.; Ho, S.-C.; Yeh, K.-Y.; Pawlak, C. R.; Chang, H.-M.; Ho, Y.-J.; Lai, T.-J.; Wu, F.-Y. *Pharmacol. Biochem. Be.* **2012**, *102*, 64. (b) Marino, M. J.; Awad, H.; Poisik, O.; Wittmann, M.; Conn, P. J. *Amino Acids* **2002**, *23*, 185.
5. Bear, M. F.; Huber, K. M.; Warren, S. T. *Trends Neurosci.* **2004**, *27*, 370.
6. Zhu, C. Z.; Hsieh, G.; EI-Kouhen, O.; Wilson, S. G.; Mikusa, J. P.; Hollingsworth, P. R.; Chang, R.; Moreland, R. B.; Brioni, J.; Decker, M. W.; Honore, P. *Pain* **2005**, *114*, 195.
7. For a recent review, see: Majo, V. J.; Prabhakaran, J.; Mann, J. J.; Kumar, J. S. D. *Drug Disc. Today* **2013**, *18*, 173.
8. (a) Ametamey, S. M.; Kessler, L. J.; Honer, M.; Wyss, M. T.; Buck, A.; Hintermann, S.; Auberson, Y. P.; Gasparini, F.; Schubiger, P. A. *J. Nucl. Med.* **2006**, *47*, 698. (b) Ametamey, S. M.; Trever, V.; Streffer, J.; Wyss, M. T.; Schmidt, M.; Blagoev, M.; Hintermann, S.; Auberson, Y.; Gasparini, F.; Fischer, U. C.; Buck, A. *J. Nucl. Med*. **2007**, *48*, 247. (c) Hintermann, S.; Vranesic, I.; Allgeier, H.; Brülisauer, A.; Hoyer, D.; Lemaire, M.; Moenius, T.; Urwyler, S.; Whitebread, S.; Gasparinia, F.; Aubersona, Y. P. *Bioorg. Med. Chem*. **2007**, *15*, 903.
9. Son, M.-H.; Kim, J. Y.; Lim, E. J.; Baek, D.-J.; Choi, K.; Lee, J. K.; Pae, A. N.; Min, S.-J.; Cho, Y. S. *Bioorg. Med. Chem. Lett.* **2013**, *23*, 1472.
10. Kim, S. H.; Na, H. S.; Sheen, K.; Chung, J. M. *Pain* **1993**, *55*, 85.
11. (a) Thompson, S. J.; Millecamps, M.; Aliaga, A.; Seminowicz, D. A.; Lowb, L. A.; Bedell, B. J.; Stone, L. S.; Schweinhardt, P.; Bushnell, M. C. *NeuroImage* **2014**, *91*, 344. (b) Kim, C.-E.; Kim, Y. K.; Chung, G.; Im, H. J.; Lee, D. S.; Kim, J.; Kim, S. J. *NeuroImage* **2014**, *91*, 311.
12. Shigemoto, R.; Nomura, S.; Ohishi, H.; Sugihara, H.; Nakanish, S.; Misuno, N. *Neuroscience Lett*. **1993**, *163*, 53.
13. Fernandez, M.; de la Cuesta, E.; Avendano, C. *Heterocycle* **1994**, *38*, 2615.
14. Muto, K.; Yamaguchi, J.; Itami, K. *J. Am. Chem. Soc*. **2012**, *134*, 169.
15. Karramkam, M.; Dolle, F.; Valette, H.; Besret, L.; Bramoulle, Y.; Hinnen, H.; Vaufrey, F.; Franklin, C.; Bourg, S.; Coulon, C.; Ottaviani, M.; Delaforge, M.; Loćh, C.; Bottlaendera, B.; Crouzela, C. *Bioorg. Med. Chem. Lett.* **2002**, *10*, 2611.
16. Chaplan, S. R.; Bach, F. W.; Pogrel, J. W.; Chung, J. M.; Yaksh, T. L. *J. Neurosci. Methods* **1994**, *53*, 55.
17. Dixon, W. J. *Ann. Rev. Pharmacol. Toxicol.* **1980**, *20*, 441.
18. Choi, Y.; Yoon, Y. W.; Na, H. S.; Kim, S. H.; Chung, J. M. *Pain* **1994**, *59*, 369.